

September 25th - 28th, 2017



Proceedings of the IASS Annual Symposium 2017
“Interfaces: architecture.engineering.science”
25 - 28th September, 2017, Hamburg, Germany
Annette Bögle, Manfred Grohmann (eds.)

Thin-shell textile-reinforced concrete floors for sustainable buildings

Will HAWKINS*, John ORR^a, Paul SHEPHERD^a, Tim IBELL^a, Julie BREGULLA^b

*Department of Architecture and Civil Engineering, University of Bath, UK
w.j.hawkins@bath.ac.uk

^a Department of Architecture and Civil Engineering, University of Bath

^b Building Technology Group, Building Research Establishment Ltd (BRE)

Abstract

Steel-reinforced concrete, cast in flat prismatic forms, dominates multi-storey building construction around the world. Despite the fluidity of the material, opportunities to create efficient geometries through manipulation of form are habitually overlooked, resulting in inefficient cracked sections, high steel requirements and large carbon footprints. This project brings together modern developments in computational design, materials and construction to propose a novel thin-shell concrete flooring system for multi-storey buildings, creating a low embodied energy and lightweight alternative to traditional reinforced concrete flat slabs. In this investigation, the performance of various shell geometries are compared using finite element analysis. A functional design is produced and found to offer reductions of 62% in embodied energy and 64% in weight compared to an equivalent flat slab.

Keywords: Concrete shells, construction, form finding, structural optimisation, textile reinforced concrete, sustainable design, finite element analysis.

1. Introduction

Developments in technology, legislation and industrial practice are significantly improving the operational energy efficiency of new buildings, making embodied materials the dominating contributor to total lifecycle energy (Sturgis and Roberts [10]). In a typical multi-storey concrete framed building, the floors are the largest consumers of material (Foraboschi *et al.* [3]) and flat slabs are often preferred due to their simple formwork and architectural flexibility. Design methods for flat slabs assume bending and shear behaviour, with large volumes of concrete ignored due to cracking in tension. It has however been shown that restraining flat slabs laterally can increase their loading capacity by three times due to an arching effect known as compressive membrane action (Ockleston [8]). This supports the hypothesis that an alternative approach to floor design, using compression shells, could significantly improve material efficiency.

2. Proposed structural system

The proposed structure features pre-cast concrete shell units supported by columns at each corner, as shown in Figure 1. Textile reinforcement provides ductility in the event of failure as well as increasing bending and tensile strength where required. Textile reinforced concrete (TRC) combines layers of flexible fibre reinforcement, typically glass or carbon, with concrete to create a composite material. It is well suited to forming thin shell structures since the reinforcement is flexible and there are no minimum cover requirements for durability. Foamed concrete is then cast onto the shells in-situ to create a level upper floor surface, provide acoustic and thermal insulation, and restrain the shell against buckling. A system of tension ties is also required to resist lateral thrust. Disproportionate collapse is avoided, since each shell acts as an independent unit.

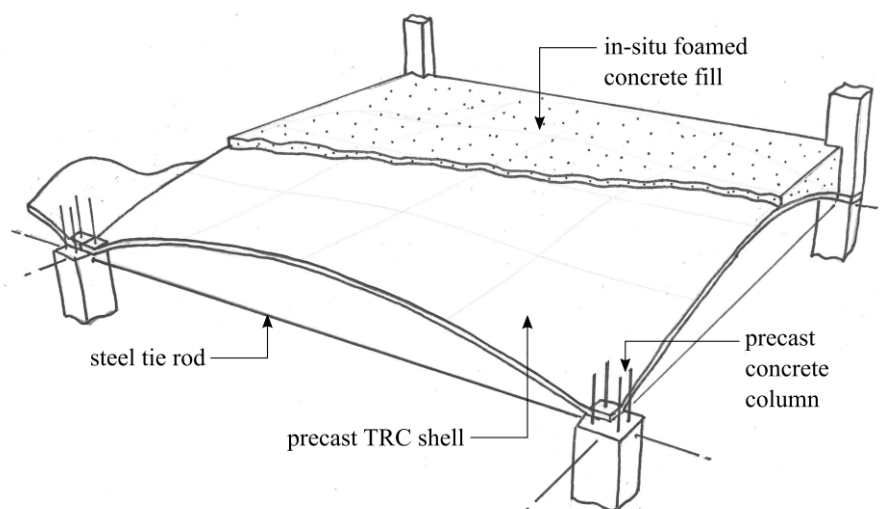


Figure 1: Components comprising the proposed flooring system

As the total depth (or rise) of the shell increases, the compressive forces in the shell and horizontal thrust decrease, reducing the required section thickness and tie strength. It is therefore proposed to integrate building services within the structural zone in order to avoid increasing overall building height.

3. Shell geometry design investigation

In order to compare the performance of a variety of different shell geometries, an investigation was carried out on shells spanning 8m between 500mm square columns. Each shell is 50mm thick and has a total structural depth of 800mm (including a minimum foamed concrete layer of 20mm).

3.1. Analysis method

In this analysis, all loads are conservatively assumed to be carried by the shell. The fill is not considered to provide any strengthening or stiffening function. The shell is modelled using triangular plate elements of constant strain, based on Kirchhoff plate theory, and is assumed to be fixed rigidly at the column interface. Horizontal movement perpendicular to the shell edge is also restrained, modelling the lateral support from a neighbouring shell with similar (symmetrical) deformation. Because of the potential geometric sensitivity of the shell structures, second order geometric non-linearities are considered in the finite element analysis. Linear-elastic material behaviour is assumed since the concrete is designed to act primarily in compression. The Young's modulus of 34GPa and Poisson's ratio of 0.2 correspond to a concrete strength class of C35/45.

The loads applied to the shell include the self-weight of the shell (density 24kN/m^3) and the fill (density 8kN/m^3) which is proportional to the local depth. A superimposed dead load of 1.0kN/m^2 is included for finishes and services, with a 3.5kN/m^2 live load accounting for typical office use in the UK (2.5kN/m^2) plus partitions (1.0kN/m^2) (British Standards Institution [1]). These loads are combined without load factors for serviceability assessment, and applied uniformly over the floor area.

Several results are calculated for comparison. The shell geometry affects the volume of the fill as well as the shell surface area, and therefore the self-weight (ω_{self}) is compared. The total strain energies from compressive (U_c), tensile (U_t) and bending (U_b) forces are calculated in order to assess the structural behaviour. Bending and axial forces are ideally minimised to reduce the required shell thickness and reinforcement. The maximum vertical deflections ($\delta_{v, \text{max}}$) and the factor of safety against buckling in the 1st mode (P_{cr}/P) are also calculated for each of the analysed shell geometries.

3.2. Shell geometries

Table 1 shows the nine shell geometries which are considered. A 275mm thick concrete flat slab is included as a reference (geometry 1), with the self-weight of the fill is ignored. This thickness was chosen based on a typical Eurocode design for the given span and loading (Goodchild [4]). Several mathematically-defined shells are also analysed. The simplest of these is a sphere (geometry 2). Three shells constructed from hyperbolic paraboloids (or ‘hypars’, distinctively used in the concrete shells of Felix Candela) are also defined. The first of these (geometry 3) features four hypars intersecting at the mid-span of the columns. The second (geometry 4) features two saddle-shaped hypars intersecting at right angles to create a groin vault. The geometry of this shell can be controlled through the ratio of the z coordinates at the mid-point (at the intersection of column diagonals) and the highest point (along the edge). In geometry 4, this ratio is 0.9. If this ratio is set to 1.0, then the shell becomes singly curved with a parabolic profile (geometry 5).

A fundamental concept in the form finding of shells is that of ‘funicular’ geometry, where a specified loading is supported by the shell entirely through membrane forces. Having no bending or compressive strength, flexible structures such as fabrics or cable-nets must always take on a funicular geometry in order to resist loads purely through tensile forces. This can therefore form the basis of a form finding approach for shells through the principle of inversion: a purely tensile geometry inverted will resist the same loads purely in compression. A form-finding method was developed which features an initially flat grid of points, aligned with the column grid, connected by springs in both the orthogonal and 45° directions (Figure 2). By applying inverted loads to the cable-net, a funicular geometry can theoretically be derived for the concrete shell. The fabric is restrained in all directions at columns, and against moving normal to the boundaries. In geometry 6, the SLS loads are applied to the cable net for form-finding, and the spring stiffness is equal in both the orthogonal and 45° directions. By varying the stiffness of the springs in each direction, the geometry can be controlled. In geometry 7, the height of the shell at the centre and at the edge is made equal by increasing the stiffness of the 45° springs, and correspondingly reducing that of the orthogonal springs.

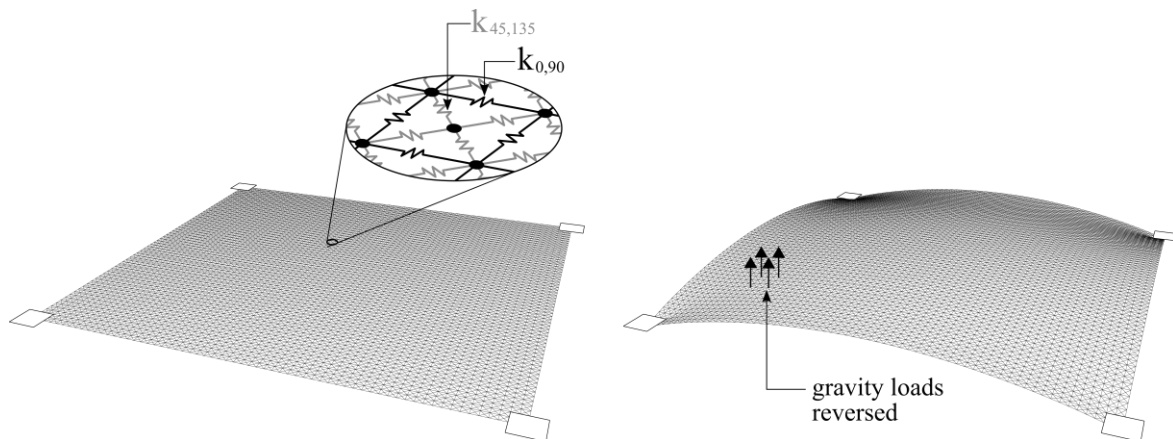


Figure 2: Form-finding with an initially flat cable-net

This form-finding method can also be used to simulate the geometry produced by using fabric-formwork, a construction technique which allows concrete to be easily cast into curved geometries (Hawkins *et al.* [7]). By setting either the 45° or orthogonal cable stiffness to zero a fabric orientated with its weave orthogonal (geometry 8) or at 45° (geometry 9) to the column grid can be modelled. The form-finding load is also changed to include only the self-weight of the shell, and lateral movement at the fabric edges is restrained. This simulates casting the shell upside-down. For practical purposes a hardening polymer resin could be applied to the fabric in this state which would be more easily inverted than a concrete shell (West [11]).

3.4. Results

Results are shown in Table 1, with the best performing shell geometry highlighted in bold. For each of the thin-shells, the self-weight was found to be significantly lower than that of the flat slab. Those shell geometries which are more dome-like (such as geometries 2, 6 and 8) require a greater volume of fill and therefore have a higher self-weight.

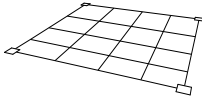
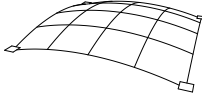
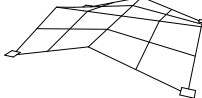
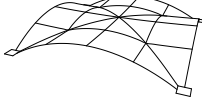
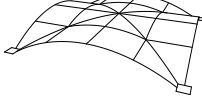
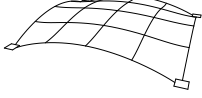
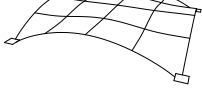
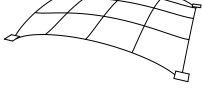
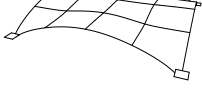
	geometry	ω_{self} [kN/m ²]	U_c [Nm]	U_t [Nm]	U_b [Nm]	U_{total} [Nm]	$\delta_{v, \text{max}}$ [mm]	P_{cr}/P
1	 flat slab (no fill, 275mm thick)	6.88	0.0	0.0	1399.1	1399.1	6.10	n/a
2	 spherical	3.42	701.8	5.7	48.4	756.0	4.46	14.2
3	 hypar quadrants	2.91	482.9	38.7	42.2	563.8	3.14	21.3
4	 hypar groin vault	2.76	440.0	13.4	38.9	492.3	6.72	27.6
5	 parabolic groin vault	2.47	347.0	3.6	20.1	370.6	4.72	21.1
6	 form-found (uniform spring stiffness)	3.01	471.8	0.9	7.0	479.6	3.39	7.6
7	 form-found (equal rise)	2.43	376.4	2.7	16.6	395.7	6.00	14.4
8	 fabric-formed (orthogonal weave)	3.15	581.5	5.2	24.3	611.0	3.83	8.4
9	 fabric-formed (45° weave)	2.48	444.4	17.0	35.5	496.8	8.48	14.6

Table 1: Geometry comparison and analysis results

The strain energy values show that the flat slab acts entirely in bending whereas the thin shells utilise primarily compressive forces. Some bending and tensile forces are present in each of the shells (Figure 3). The form-found geometries 6 and 7 have the smallest non-compressive forces, suggesting efficient shell behaviour, however the bending-free state of the hanging cable net is not perfectly reproduced. This is because the shell differs from the cable-net form-finding structure due to its bending stiffness, material properties (including Poisson's ratio) and rotationally fixed column supports. Although the mathematically defined geometries (2-5) generally feature more bending and tensile forces than the form-found shells, this is not the case for the parabolic groin vault (geometry 5).

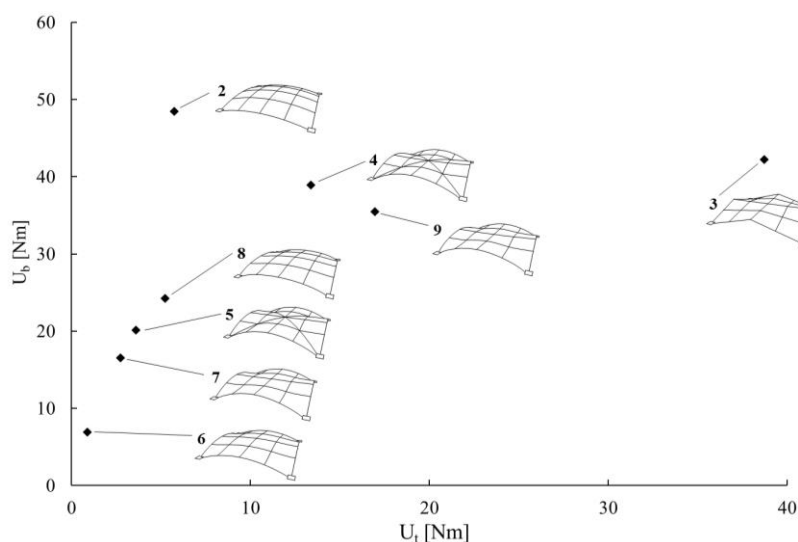


Figure 3: Bending and tensile strain energy for thin-shell geometries

The maximum vertical deflection varies considerably between shell geometries. Since the flat slab acts entirely in bending and shear, significant cracking will occur and as such the deflection calculated in this analysis is likely to be a considerable under-estimate. A more detailed which includes the effects of creep and shrinkage as well as non-rigid supports would be required to accurately assess the long-term deflection of the shells.

The three shells which show the highest buckling resistance (geometries 3, 4, and 5) are similar in that they all have discontinuities in surface curvature (creases) in their geometry, thus creating ‘ribs’ of locally increased stiffness.

4. Ultimate limit state

4.1. Analysis method

In order to quantify the possible savings in weight and embodied energy over traditional concrete floor systems, a more detailed investigation considering real-world design criteria is required. The analysis conditions are therefore modified to simulate a worst-case design scenario in the following ways:

- Load factors of 1.35 and 1.5 applied to dead and live loads respectively.
- Four patterns of live loading applied (as shown in Figure 6).
- Lateral and rotational restraint of column head removed.
- Rotational stiffness of the column included (equivalent to a 3.5 m tall pin-ended column).
- Perpendicular support along shell edges removed (simulating a single shell in isolation).
- Differential settlement of 10mm applied to opposite columns, as an imposed vertical displacement.

With the lateral support at the columns removed, the horizontal displacement at the columns is now governed by the stiffness and prestress of the steel ties. Ties are assumed to be round steel (Young modulus 210GPa) with a diameter of 40mm, and the tie prestress is adjusted to a value where there is no lateral movement at an average between the maximum (factored full live load) and minimum (unfactored self-weight only) loads. The vertical location of the ties can similarly be adjusted to control the bending moment applied to the column, and this was therefore tuned in order to produce no support moment at the average load.

A method of calculating the section utilisation through linear interpolation between key values, adapted from Scholzen *et al.* [9], is adopted for evaluation of strength performance. Utilisation is calculated from combined axial and bending forces, and is a function of the angle between the principle stress direction and the reinforcing mesh (which is orientated with the column grid). Typical values for the strength ($\sigma_{u, \text{reinf}} = 1400\text{N/mm}^2$) and stiffness ($E_{\text{reinf}} = 80\text{kN/mm}^2$) of AR-glass reinforcing mesh are assumed (Gries *et al.* [5]). A conservative modelling approach is adopted based on linear elastic concrete behaviour in compression, zero tension, and failure at first crushing of the concrete at a strain of $\epsilon_{u, \text{conc}} = 0.35\%$ and stress of 23.3MPa (C35/45 concrete with partial safety factor of 1.5 (British Standards Institution [2])), as shown in Figure 4. The predictions were checked against preliminary experimental results on TRC sections by the principle author and found to be suitably conservative. The chosen section is 50mm thick and includes a top and bottom layer of orthogonal mesh reinforcement under 5 mm of concrete cover. The total reinforcement volume fraction is 2%. The design compressive, tensile and bending strengths of the section, in the reinforcement directions, are 1166.6kN/m, 466.6kN/m and 6.5kN respectively based on the assumptions described.

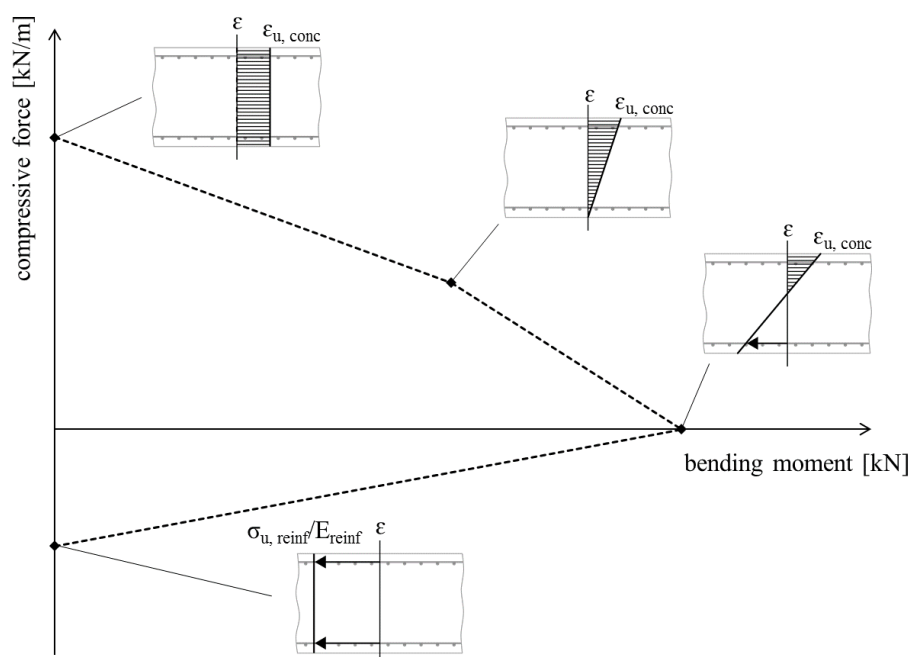


Figure 4: Assumed failure surface for utilisation calculation

4.2. Results

Figure 5 shows a histogram of the distribution of section utilisation over the shell area for each of the shells considered. In all cases, regions of the shell (typically near the corner supports) show utilisation values greater than 1, indicating that a stronger section is required locally. Similarly, material could potentially be removed from areas where the utilisation is less than 1. A variable shell thickness would therefore be an advisable design refinement which could be easily integrated into the layering process of the TRC shell.

The shell with the lowest bending and tensile strain energy in the idealised modelling scenario (geometry 6) does not out-perform the other shell geometries in this worst-case analysis. The shell with the smallest area of over-utilisation is the parabolic groin vault (geometry 5), where only 1.8% of the shell requires strengthening. The average utilisation is also smallest for this shell geometry, at 44.1%, suggesting significant material savings could be made through design refinement.

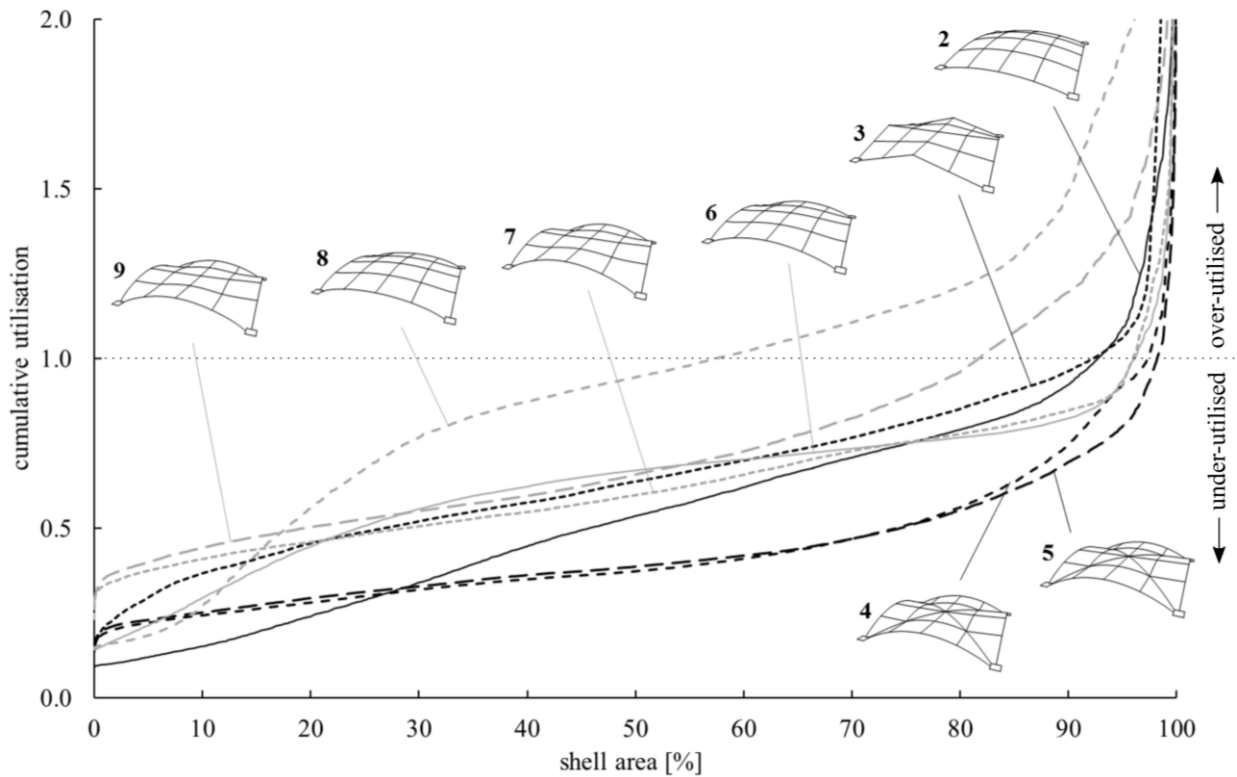


Figure 5: Histogram showing section utilisation envelope by area

The distribution of utilisation for the parabolic groin vault (geometry 5) is shown in Figure 6. Peak utilisation values occur at the column corners and are dependent on the size of the analysis mesh. The maximum force in the steel tie rods was 364kN, giving an acceptable stress of 289N/mm² in the steel.

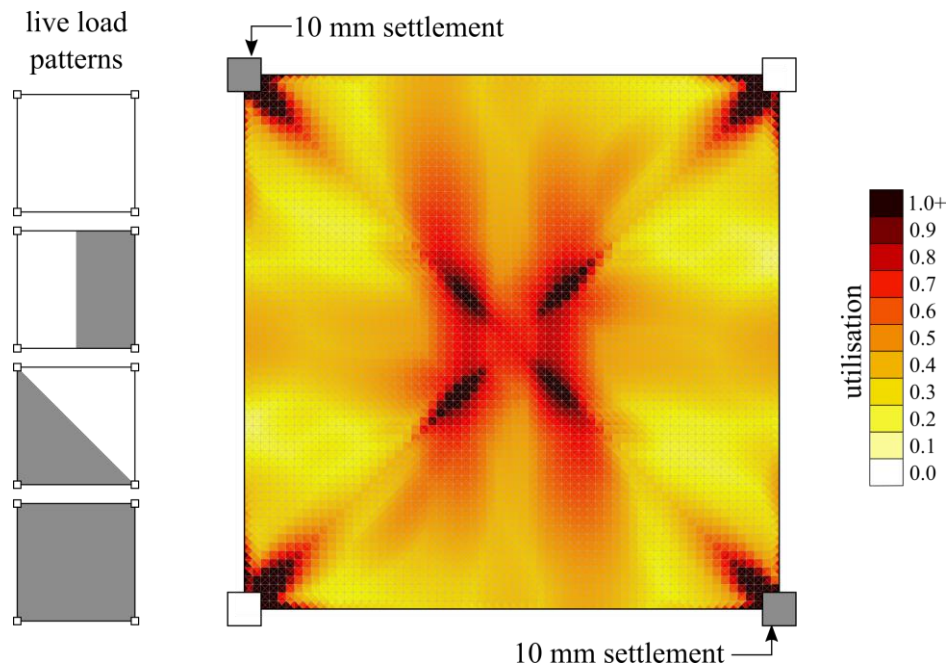


Figure 6: Live load patterns (left) and section utilisation envelope (right) for shell geometry 5

5. Discussion

5.1. Shell geometry selection

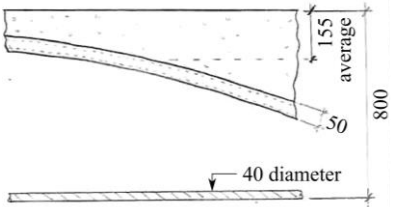
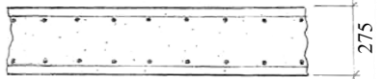
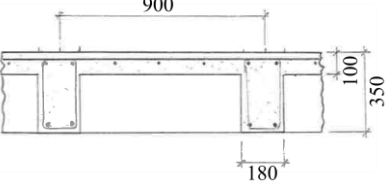
The shells which show the smallest amounts of bending and tension forces in Section 3 (idealised boundary conditions with uniform serviceability loading) are not necessarily the best performing in the worst-case scenario. Understanding support and loading conditions is therefore of primary importance for design. This contrasts with large-span roof structures for example, where supports are comparatively rigid and self-weight is often the dominant loadcase.

The formwork for shell geometries 3, 4 and 5 (all hypars) can be constructed using straight elements, and the fabric-formed shells potentially have even simpler formwork consisting of a rigid outer frame and fabric. For practical purposes, a shell geometry should be chosen which combines efficient structural performance with construction simplicity. The results of this investigation suggest that the parabolic groin vault (geometry 5), having the lowest self-weight, greatest potential for shell thickness reduction and a simple geometry for construction, would be a good candidate for further development.

5.2. Environmental comparison with traditional concrete floors

The parabolic groin vault (geometry 5) is compared with two common concrete floor structures with equivalent span and loadings. These were specified according to EC 2 using sizing tables (Goodchild [4]). Values of embodied energy for each material were taken from the ICE Inventory of carbon and energy (Hammond and Jones [6]). The self-weight and embodied energies are compared in Table 2.

Table 2: Self-weight and embodied energy comparison

construction	component	material embodied energy [MJ/kg]	equivalent density [kg/m ³]	volume per floor area [m ³ /m ²]	weight [kN/m ²]	embodied energy [MJ/m ²]
	C35/45 (shell)	0.93	2400	0.0500	1.20	112
	glass fibre textile	25.58	2800	0.0010	0.03	72
	foamed concrete fill	1.22	800	0.1550	1.24	151
	steel ties	17.40	7840	0.0003	0.02	43
	total: 2.49					total: 377
	C30/37	0.86	2400	0.2750	6.60	568
	reinforcing steel	17.40	90	0.2750	0.25	431
total: 6.85						total: 998
	C30/37	0.86	2400	0.1900	4.56	392
	reinforcing steel	17.40	110	0.1900	0.21	364
	total: 4.77					total: 756

The proposed shell floor shows reductions of 64% in weight and 62% in embodied energy compared to the flat slab, and 48% and 50% respectively compared to the waffle slab. These savings would be further increased through refinement of the shell thickness, as well as reductions in column and foundation loads throughout the building.

5.3. Conclusions & future work

A novel structural system is proposed combining thin TRC shells with a foamed concrete fill and steel ties. The performance of the shell is sensitive to the geometry as well as the loading and boundary conditions, which are complex and varied in a floor structure. This preliminary investigation has demonstrated that a singly curved parabolic groin vault, with simple construction geometry, can be used to create a viable thin-shell floor structure with significant reductions in self-weight (-64%) and embodied energy (-62%) compared to traditional flat slabs. This clearly demonstrates the improved material efficiency of shells which utilise membrane action over slabs and beams acting in bending and shear for concrete structures.

Future work by the authors will explore and resolve further technical details, practicalities and design refinements for the proposed system. These include the effects of initial imperfections, variable section thicknesses, non-linear material behaviour, point loadings and stability loads. A programme of prototyping and physical testing is also being undertaken.

Acknowledgements

This research is supported by the EPSRC Centre for Decarbonisation of the Built Environment (dCarb) [grant number EP/L016869/1] and a Building Research Establishment (BRE) Scholarship.

References

- [1] British Standards Institution, 2002. UK National Annex to Eurocode 1: Actions on structures. *Part 1-1: General actions — Densities, self-weight, imposed loads for buildings*. London: British Standards Institution.
- [2] British Standards Institution, 2008. Eurocode 2: Design of concrete structures. *Part 1-1: General rules and rules for buildings*. London: British Standards Institution.
- [3] Foraboschi, P., Mercanzin, M. & Trabucco, D., 2014. Sustainable structural design of tall buildings based on embodied energy. *Energy and Buildings*, 68(Part A), pp. 254-269.
- [4] Goodchild, C.W., R M; Elliot K S, 2009. *Economic concrete frame elements to Eurocode 2*. Surrey, UK: The Concrete Centre.
- [5] Gries, T., Roye, A., Offerman, P., Engler, T. & Peled, A., 2006. Textiles. In: W. Brameshuber, ed. *Textile Reinforced Concrete - State-of-the-Art Report of RILEM TC 201-TRC*. RILEM.
- [6] Hammond, G. & Jones, C., 2011. Inventory of carbon & energy Version 2.0 (ICE V2.0). *Department of Mechanical Engineering, University of Bath, Bath, UK*.
- [7] Hawkins, W., Herrmann, M., Ibell, T., Kromoser, B., Michalski, A., Orr, J., Pedreschi, R., Pronk, A., Schipper, R., Shepherd, P., Veenendaal, D., Wansdronk, D. & West, M., 2016. Flexible formwork technologies - a state of the art review. *Structural Concrete*, 17(6), pp. 911 - 935.
- [8] Ockleston, A., 1958. Arching action in reinforced concrete slabs. *The Structural Engineer*, 36(6), pp. 197-201.
- [9] Scholzen, A., Chudoba, R. & Hegger, J., 2015. Thin-walled shell structures made of textile-reinforced concrete: Part II. *Structural Concrete*, 16(1), pp. 115-124.
- [10] Sturgis, S. & Roberts, G., 2010. *Redefining zero: Carbon profiling as a solution to whole life carbon emission measurement in buildings*. London: RICS Research.
- [11] West, M., 2009. *Thin shell concrete from fabric molds* [Online]. Available from: <http://www.fabwiki.fabric-formedconcrete.com> [Accessed March 2017].